Empirical Study of Sediment-Filled Basin Response: The Case of Taipei City

Vladimir Yu. Sokolov, Chin-Hsiung Loh, M.EERI, and Kuo-Liang Wen

We analyze the site response of the Taipei basin using the records obtained by the Taiwan Strong Ground Motion Instrumentation Program (TSMIP) network. Records of 66 earthquakes of M=2.6-6.5 with a hypocentral depth varying from 1 km to 118 km and hypocentral distances of up to 150 km are studied for 35 stations located within this triangle-shaped alluvium structure. The site response is obtained in terms of spectral ratios calculated by dividing of the site spectrum by the reference spectrum estimated for a hypothetical "very hard rock" site. The recently developed empirical source scaling and attenuation models for the Taiwan region are used for the reference spectra calculation. This approach allows us to evaluate the variability of spectral ratios due to uncertainties introduced by source and propagation path effects and variability in the site response itself. The characteristics of site response in the Taipei basin depend on the properties of soil deposits and, in general, may be described by 1-D models. However, there are some peculiarities of spectral ratios that show the influence of subsurface topography.

INTRODUCTION

It is well understood that near-surface geological conditions strongly influence earthquake ground motion at a particular site, and the building codes used in earthquake-prone countries take into account the effect of local site conditions by using simplified site categories. Recent destructive earthquakes, including the 1985 Michoacan earthquake in Mexico, the 1988 Spitak earthquake in Armenia, the 1989 Loma Prieta and the 1994 Northridge earthquakes in California, and the 1997 Hyogo-Ken Nanbu (Kobe) earthquake in Japan, reveal the necessity to re-evaluate the building code provisions for site effect because the earthquakes were more severe than the provisions allowed for. It is believed that the local site effect is one of the major factors controlling the damage during these events (e.g., Seed et al. 1987, Borcherdt et al. 1989, Hanks and Brady 1991, Stewart et al. 1994, Irikura et al. 1996). Among many factors determining the site response to earthquake ground motion (see, for example, Aki 1988, for review) the influence of laterally irregular geological structures — sediment-filled valley or basin — may play a key role in site amplification and damage distribution (e.g., Yegian et al. 1995, Irikura et al. 1996, and Akamatsu et al. 1998). Many urban areas are situated on deep sediment-filled basins, and therefore the study of the features of basin response is very important to mitigate damage during an earthquake.

Several studies have been devoted to develop models for two- and three-dimensional structures (e.g., Lee 1984, Bard and Bouchon 1985, Bard and Gariel 1986, Sanchez-Sesma et al. 1988, Graves and Clayton 1992, Papageorgiou and Kim 1993, and Rodriguez-Zuniga et al. 1995; see also Bard 1995, for review) and to compare theory and observation (see Kudo 1994, for recent review; Campillo et al. 1988, Papageorgiou and Kim 1991, Hisada et al. 1993, Chavez-Garcia et al. 1995, Irukura et

(VYS, C-HL) NCREE, 200, Sec. 3, Hsinhai Rd., Taipei, Taiwan
(K-LW) Institute of Earth Sciences, Academia Sinica, P.O. Box 1-55, Nankang, Taipei, Taiwan

by source and propagation path effects and variability in the site response itself, may be described in terms of random variable characteristics and further used along with source scaling and attenuation models when estimating seismic hazard. The use of spectral amplification functions obtained using this approach showed (Sokolov 1997, 1998a) that the estimations are consistent with the available geotechnical data (for example, thickness of soil deposits). They produce a reliable prediction of ground motion parameters in the Caucasus region, when used in conjunction with the corresponding regional source scaling and attenuation models for the hard rock.

We used the technique to study the seismic response of the Taipei basin. The large number of ground-motion acceleration recordings, which were obtained during the execution of the Taiwan Strong Motion Instrumentation Program (TSMIP) since 1991 (Kuo et al. 1995), provide an opportunity to study both regional source scaling and attenuation models for the Taiwan region, as well as local characteristics of soil response in the Taipei basin where more than forty stations are currently in operation. The results of the previous researches of earthquake ground motion peculiarities in the Taipei basin (Kuo et al. 1995, Wen et al. 1995, Loh et al. 1998, and Wen and Peng 1998a,b) showed that, although the Taipei basin is not a large area, it reveals a large variation in ground-motion characteristics (amplitude and shape of site-amplification functions, dominant frequencies, response spectra, etc.). These characteristics depend on the geotechnical properties at the site, location of the station, and the parameters of the earthquakes. However, the records of only two (Loh et al. 1998) or three (Wen et al. 1995) earthquakes were used, and spectral amplification within a limited low-frequency band (0.25-3 Hz) has been studied (Wen and Peng 1998a). The purpose of this article is to study the variation of local site effect in different areas of the sediment-filled valley — the Taipei basin — during earthquakes that vary in magnitude, focal depth, and distance. The spectral amplification curves were obtained for the sites within the Taipei basin at frequencies of engineering interest ($0.4 \leq f \leq 12$ Hz), using the records obtained from 66 earthquakes ($2.6 \leq M \leq 6.5$) with hypocentral distances of up to 150 km. The reliability of the site-amplification data is estimated by comparison with the results of 1-D mathematical modeling. This work also may be considered as a study of the effectiveness of the employed methodology.

GEOLOGICAL STRUCTURE OF THE TAIPEI BASIN

The Taipei basin is a triangular alluvium structure, and the area (about 240 square kilometers) is almost flat at an altitude above sea level of less than 20 meters. The subsurface geology has been established by boring, electrical and seismic prospecting (Lee et al. 1978, Wang-Lee and Lin 1987, Fei and Lai 1994, and Wang et al. 1994). The geological structure inside the basin consists of Quaternary layers above Tertiary base rock. Figure 1 shows a scheme of the Taipei basin, a cross section through the basin, and stations of the Taipei strong motion observation network whose recordings are used in this study.

The stratigraphic formation of the Quaternary layers are, in descending order, surface soil, the Sungshan Formation, the Chingmei Formation, and the Hsinchuang Formation. The Sungshan Formation is composed mainly of alternating beds of silty clay and silty sand, and covers almost the whole Taipei basin. The Chingmei Formation is a fan-shaped body of conglomerate deposits. The Hsinchuang Formation, recently separated into the Wuku and Panchiao Formations, consists of bluish-grey and clayey sand with some conglomerate beds. The average P- and S-wave velocity structures for the Taipei basin are given in Table 1 and are results taken from the reflection seismic survey carried out for the entire Taipei area by Wang et al. (1996). The bottom depth contour map of the soft Sungshan Formation is shown in Figure 2.

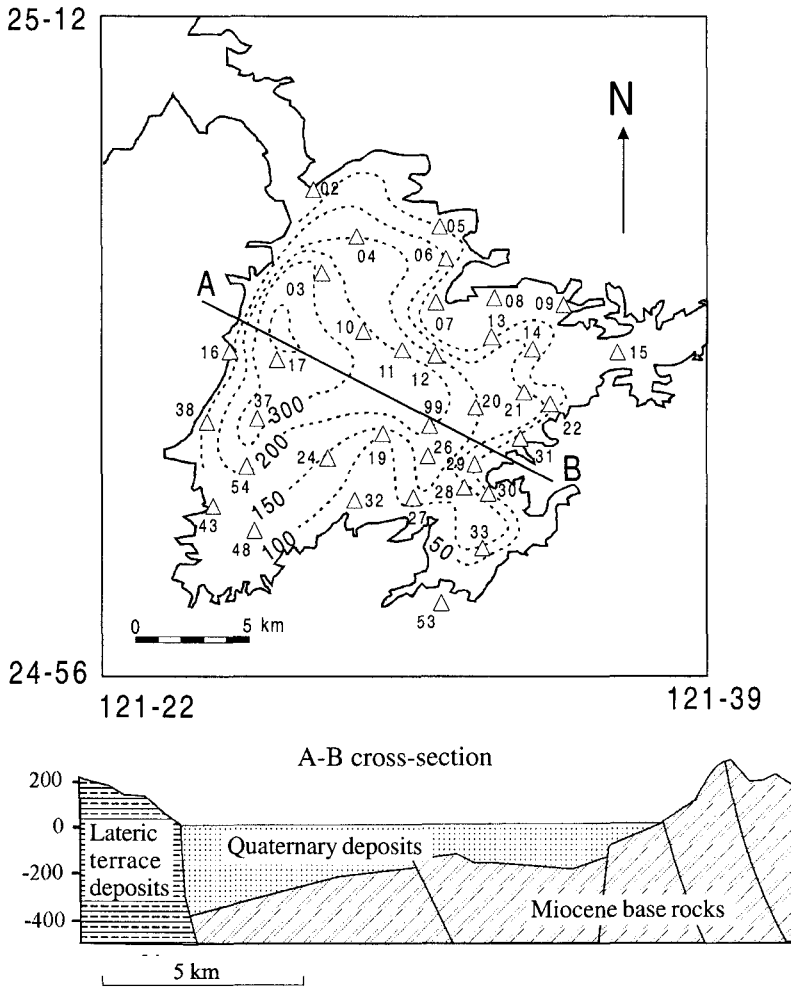

Figure 1. Map of the Taipei basin and location of TSMIP network stations (triangles), recordings of which were used in this study. Numbers indicate the station codes. The dotted contours show the depth in meters to the base rock surface in the Taipei basin.

Table 1. Velocity structure of the Taipei Basin (Wang et al. 1996)

Formation	depth, meters		Vp	Vs
	Northwest	Southwest	(m/sec)	(m/sec)
Sungshan	0-25	0-15	450	170
	20-50	15-35	1500	230
	50-100	35-50	1600	340
Chingmei	100-160	50-100	1800	450
Wuku	160-320	100-200	2000	600
Panchiao	320-400	200-250	2200	650
Basement			3000	1200

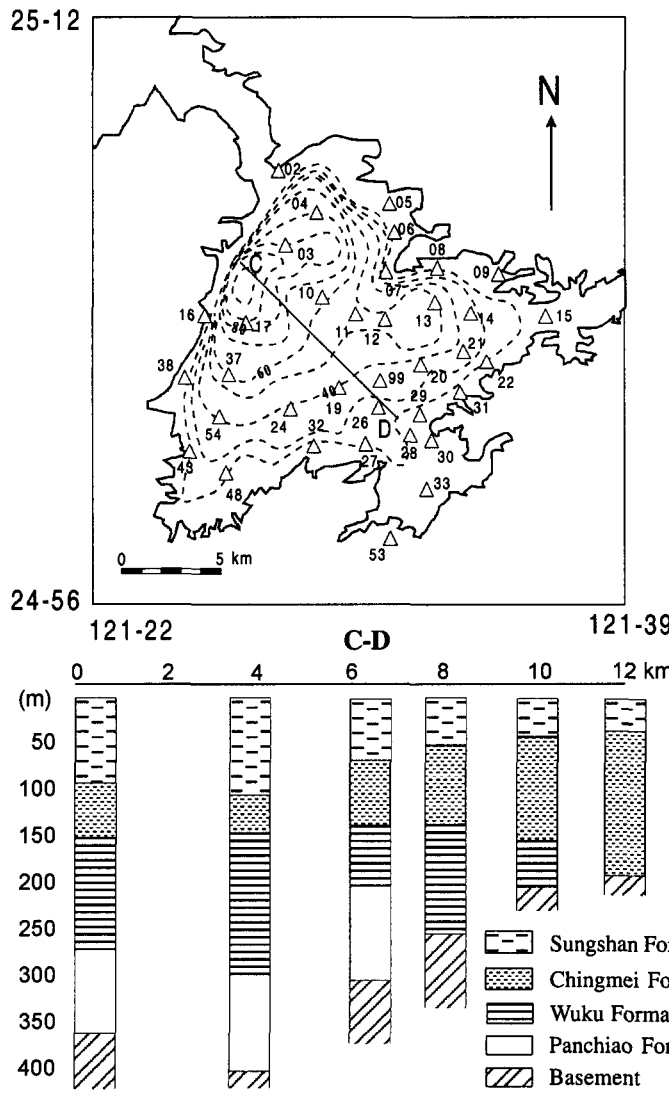

Figure 2. Contour map showing the depth in meters to the bottom of Sungshan Formation in the Taipei basin and models of Quaternary deposit columns (Wang et al. 1996).

TSMIP NETWORK AND EARTHQUAKE DATA

The Taiwan Strong Motion Instrumentation Program (TSMIP, Kuo et al. 1995) is conducted by the Seismological Observation Center of the Central Weather Bureau, Taiwan, R.O.C. The main purpose of this program is to study the characteristics of ground motion in different geological conditions, and the responses of various types of man-made structures. The program installed up to 600 digital free-field strong-motion instruments, and about 100 stations are already in operation in the Taipei area, including 43 stations within the Taipei basin. (In Figure 1 triangles denote the station used in this study and the number near the station gives the station code.) Each station includes one strong-motion instrument—a force-balanced three-component accelerometer. The recorder has 16-bit resolution, which enables the apparatus to record high-resolution ground motion within ± 2 g and with a pre-event and post-event memory. All stations

have AC power, and when the power system is shut down by an earthquake or other problem, the internal DC power of the recording system can still operate for about four days.

By the end of 1998, many earthquakes had been recorded by this network since its installation. The events used in this study (and that triggered three or more stations) are listed in Table 2. The distribution of the epicentres is shown in Figure 3. Source parameters of these events are determined by the local seismic network of the Central Weather Bureau, Taiwan. The whole data set includes 66 earthquakes, the magnitude range is from 2.6 to 6.5 on the local magnitude scale, the hypocentral depth covers 1 km to 118 km, and the hypocentral distance range is from 10-15 km to 150-160 km.

METHOD OF ANALYSIS

The site/bedrock spectral ratios (SBSR) are obtained by dividing the actual Fourier amplitude spectrum by the spectrum that is modeled for a hypothetical "very hard rock" (VHR) site. The advan-

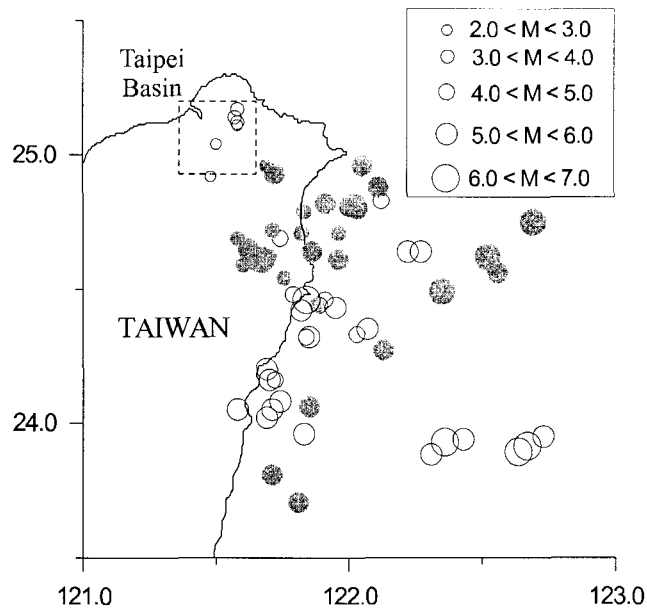

Figure 3. Distribution of epicenters of the earthquakes, recordings of which are used in this study. The open circles indicate shallow earthquakes (hypocentral depth H ≤ 35 km), and the shadow circles indicate deep (H > 35 km) events.

Table 2. Earthquakes used in this study and that triggered three or more stations

Events	Origin date	Epicentre		Local Magnitude	Depth (km)	Stations (code) used
		Lattitude, N	Longitude, E			
1	2	3	4	5	6	7
1	January 23, 1993	24.08	121.74	5.40	28.5	02, 03, 09, 16, 20, 22, 26, 27, 28, 31
2	July 4, 1993	24.88	122.11	5.69	118.0	09, 13, 14, 21, 30, 31
3	January 20, 1994	24.06	121.85	5.58	49.5	09, 13, 15, 20, 21, 22, 26, 32, 33, 43, 48, 53
4	February 1, 1994	24.75	122.69	6.13	115.0	13, 21, 26, 38, 54
5	April 18, 1994	24.8	122.03	5.08	94.9	21, 22, 32, 37, 43, 48
6	April 30, 1994	24.35	122.07	5.04	3.9	17, 22, 32, 43, 48
7	June 5, 1994	24.46	121.84	6.20	5.3	02, 03, 05, 06, 07, 09, 10, 11, 12, 13, 15, 19, 20, 21, 22, 24, 26, 28, 29, 30, 31, 32, 37, 43, 48

Table 2. (continued)

1	2	3	4	5	6	7
8	June 5, 1994	24.42	121.82	5.02	1.0	32, 43, 48
9	June 5, 1994	24.48	121.79	4.73	1.1	09, 22, 43, 48
10	June 6, 1994	24.43	121.95	5.06	3.5	09, 22, 26, 32, 43, 48
11	October 12, 1994	24.81	122.00	5.67	73.1	02, 05, 06, 08, 09, 10, 11, 12, 13, 14, 16, 21, 22, 29, 31, 32, 37, 38, 48, 54
12	October 28, 1994	24.64	122.27	5.66	2.0	05, 06, 13, 14, 15, 20, 21, 22, 24, 26, 27, 32, 37, 38, 48, 53
13	November 10, 1994	24.92	121.48	2.92	11.8	32, 33, 48
14	November 26, 1994	24.64	122.22	5.54	3.8	11, 32, 33, 43, 48, 53
15	February 23, 1995	24.2	121.69	5.77	21.7	02, 03, 04, 05, 06, 07, 08, 09, 10, 11, 12, 15, 15, 21, 27, 29, 30, 31, 32, 37, 38, 43, 54
16	March 24, 1995	24.64	121.86	5.64	76.0	02, 03, 05, 06, 07, 08, 09, 10, 11, 12, 14, 15, 16, 21, 24, 27, 29, 30, 31, 32, 37, 38, 53, 99
17	April 24, 1995	24.65	121.62	5.28	63.1	02, 05, 09, 10, 11, 12, 14, 15, 21, 29, 30, 32, 37, 38, 53, 99
18	June 25, 1995	24.61	121.67	6.50	39.9	02, 04, 05, 07, 08, 09, 10, 11, 12, 15, 16, 19, 20, 21, 24, 27, 28, 29, 30, 31, 32, 33, 37, 38, 43, 53, 99
19	July 7, 1995	24.62	121.70	4.62	44.7	32, 48, 53
20	July 14, 1995	24.32	121.85	5.80	8.8	02, 03, 06, 07, 08, 09, 11, 12, 14, 20, 21, 22, 30, 38, 43, 48, 53, 99
21	July 28, 1995	24.71	121.96	4.71	71.5	22, 32, 53
22	August 20, 1995	24.69	121.58	4.92	56.9	02, 07, 08, 09, 10, 11, 12, 14, 15, 20, 21, 22, 30, 31, 32, 37, 38, 43, 53, 99
23	December 1, 1995	24.61	121.64	5.72	45.1	04, 05, 06, 07, 08, 09, 10, 11, 12, 14, 16, 20, 21, 22, 24, 27, 30, 32, 37, 38, 43, 53, 99
24	December 18, 1995	24.02	121.69	5.80	22.1	09, 12, 30, 32, 43, 48, 53
25	December 20, 1995	24.05	121.71	5.06	33.7	32, 43, 53
26	January 22, 1996	24.93	121.72	5.11	66.9	02, 05, 06, 07, 08, 09, 13, 20, 22, 29, 30, 32, 37, 38, 43, 48, 53, 99
27	March 5, 1996	23.93	122.36	6.40	6.0	15,16, 20, 22, 99
28	July 27, 1996	24.33	122.03	4.82	7.2	09, 12, 13, 14, 21, 22, 26, 30, 99
29	July 29, 1996	24.49	122.35	6.14	65.7	02, 06, 07, 08, 09, 10, 11, 12, 13, 14, 15, 16, 17, 19, 21, 22, 24, 26, 29, 30, 31, 37, 38, 99
30	November 26, 1996	24.16	121.70	5.35	26.2	02, 05, 08, 09, 11, 12, 13, 14, 21, 22, 26, 29, 30, 32, 33, 37, 38, 43, 54, 99
31	March 24, 1997	24.16	121.72	4.83	29.1	21, 26, 32, 43, 53, 99
32	April 2, 1997	24.69	121.74	4.33	12.0	29, 32, 33, 43
33	April 13, 1997	23.81	121.71	5.56	45.5	21, 24, 26, 32, 33, 53
34	May 15, 1997	24.79	121.93	4.88	93.0	21, 37, 43, 53
35	June 24, 1997	25.12	121.58	3.70	8.6	02, 03, 05, 06, 07, 08, 09, 10, 11, 12, 14, 17, 20, 21, 26, 29, 31, 32, 99
36	July 15, 1997	24.62	122.52	6.10	86.6	03, 12, 20, 21, 26, 29, 31, 32, 33, 37, 99
37	March 4, 1998	25.04	121.50	2.59	5.7	11, 24, 26, 99
38	May 9, 1998	24.82	121.91	5.38	83.6	02, 06, 10, 12, 13, 14, 19, 21, 22, 26, 30, 31, 32, 33, 43, 53, 54, 99

tages to this technique are as follows. In the traditional spectral-ratio method, the choice of reference site may be very difficult: the reference site should be located on a hard-rock outcrop not far from the sedimentary site, and it should provide records of almost every earthquake. However, a regionally appropriate source-scaling and attenuation model for a "hard rock" site is usually available or may be derived on the basis of earthquake recordings. The use of the model makes it possible to analyze all

records. The SBSR function reflects an intrinsic variability in the site response itself (by virtue of different incidence angles, back-azimuths, etc.) and the source and path effects. The results in conjunction with the same "hard rock" spectral model used can then be incorporated into "site-dependent" seismic hazard assessment.

There are, however, some limitations. In this study we used a simple ω-squared point-source spectral model that may be inadequate in the case of a large nearby event. A finite-fault spectral model should be useful in this case. The other related problems and assumptions will be discussed below. The approach used in this study is similar to the method proposed by Su et al. (1998). They estimated the S-wave site response relative to a regional layered crustal model. In this case, however, it is necessary, though not always possible, to choose a proper regional velocity model. In addition, a complicated computational procedure that includes synthetic Green's function must be employed. This technique seems to be useful when computing site-specific strong-motion estimates for a single event, but it is not suitable for probabilistic seismic hazard assessment.

The seismic network in the Taipei basin, despite a large number of the stations, could not provide the one that is suitable to be accepted, undoubtedly, as a "hard-rock reference" station. The tightly built Taipei valley is surrounded by hills formed by weathered sandstones and shales. The stations outside the valley are located on the hill slopes or in the narrow canyons on shallow soft alluvium and reveal high-resonance peaks in the spectra of the records. In the previous research the site response was studied with respect to the TAP16 site, which is near the edge of the basin (Wen and Peng 1998a) or the mean spectrum averaged from all records of a single earthquake (Loh et al. 1998). In this study we used a hypothetical "very hard rock" spectrum as a reference spectrum. The empirical ω-squared for the Taiwan region has recently been developed (Sokolov et al., 2000) on the basis of 1070 acceleration records obtained during 81 earthquakes ($5.1 \le M \le 6.5$) that occurred since 1991 at distances of up to 200 km, and is used for the determination of reference spectra in this study.

The general model of radiated spectra, describing the Fourier acceleration spectrum A at frequency f, can be expressed in the following way (Boore 1983)

$$A(f) = (2\pi f)^2 \, C \, S(f) \, D(R, f) \, I(f) \tag{1}$$

where C is the scaling factor, $S(f)$ is the source spectrum, $D(R, f)$ is the attenuation function, and $I(f)$ represents the frequency-dependent site response. Actually, the function $I(f)$ depends also on the amplitude of excitation and, therefore, earthquake magnitude and distance. The scaling factor is given by

$$C = (\langle R_{\theta\phi} \rangle \, F \, V) / (4\pi \rho \, \beta^3 R^b) \tag{2}$$

where $\langle R_{\theta\phi} \rangle$ is the radiation coefficient, F is the free surface amplification, V represents the partitions of the vector into horizontal components, ρ and β are the density and shear velocity in the source region, respectively, b is the coefficient of geometrical spreading model (to be discussed later), and R is the hypocentral distance.

A commonly used source function $S(f)$ in the Brune model (Brune 1970) is

$$S(f) = M_0 / [\, 1 + (f/f_0)^2 \,] \tag{3}$$

For the Brune model, the source acceleration spectrum at low frequencies increases as f^2 and approaches a value determined by f_0 (corner frequency) and M_0 at frequencies $f > f_0$. The value of f_0 can be found from the relation $f_0 = 4.9 \times 10^6 \, \beta \, (\Delta\sigma / M_0)^{1/3}$. Here $\Delta\sigma$ is the stress parameter in bars, M_0 is the seismic moment in dyne-cm and β in km/sec. The level of the spectrum remains approximately constant for frequencies above f_0 until the cut-off frequency f_{max} is approached. The amplitude of the spectrum decays rapidly at frequencies above f_{max}.

The function $D(R, f)$ accounts for frequency-dependent attenuation that modifies the spectral shape. It depends on the hypocentral distance (R), regional crustal material properties, the frequency-dependent regional quality factor Q, and f_{max}. These effects are represented by the equation

$$D(R, f) = exp\ [-\pi f R / Q(f) \beta]\ P(f, f_{max}) \quad (4)$$

where $P(f, f_{max})$ is a high-cut filter. Two forms of the P-filter are used: the Butterworth filter (Boore 1983)

$$P(f) = [1 + (f/f_{max})^8]^{-1/2} \quad (5)$$

and that proposed by Anderson and Hough (1984)

$$P(f) = exp\ (-\pi \kappa f) \quad (6)$$

The f_{max} filter produces a more rapid spectral decay than κ (kappa) filter.

When determining the sourc-scaling and attenuation model for the Taiwan region, we used the following procedure (Sokolov et al. 2000). The whole data set was divided into three groups by meaning of magnitude, namely $5.1 \le M_L \le 5.5$, $5.6 \le M_L \le 6.0$, $6.1 \le M_L \le 6.5$ and shallow (hypocentral depth $H \le 35$ km) and deep ($H > 35$ km) events were selected in every group. The difference between spectral amplitudes at a given frequency for every group, besides source-dependent variations, is caused by distance-dependent attenuation and site-dependent amplification factor. When partially removing spectral amplitude and shape modification by multiplying by $R\ exp\ [\pi f R / Q(f) \beta]$ (i.e., recalculating to "reference distance" $R = 1$ km), the scatter of spectral amplitudes, ideally, is determined only by source- and site-dependent factors. Let us suppose that, for the most considered events, the site amplification does not depend on shaking intensity. Therefore, the proper attenuation model should provide minimum dispersion of the spectral amplitudes at all considered frequencies at "reference distance." It has been found that frequency-dependent attenuation of spectral amplitudes with distance may be described using quality factor $Q = 225 f^{1.1}$ both for deep and shallow earthquakes. When including into analysis the data from earthquakes of magnitudes $4.5 \le M_L \le 5.0$ (Sokolov et al., 1999), we have found that quality factor $Q = 125 f^{0.8}$ should be used for shallow events. The result are consistent with the previous studies of the factor Q in the Taiwan region (Wang 1993). When considering geometrical spreading in the form $1/R^b$ (Equation 2), attenuation of the direct waves is described using $b = 1.0$ for $R < 50$ km; for a transition zone where a direct wave is joined by postcritical reflections from mid-crustal interfaces and the Moho-doscontinuity ($50 < R < 150$-170 km) $b = 0.0$, and attenuation of multiply reflected and refracted S-waves is described by $b = 0.5$ for $R > 170$ km.

We did not consider soil effect therefore the spectra at "reference distance," averaging the variety of site conditions from rock site to soft soil of different thickness, correspond to so-called "average soil." In the case of "bedrock" or "very hard rock" (VHR) site (factor $I(f) = 1$, Equation 1) the spectral amplitudes at low frequencies are proportional to seismic moment M_0 and the high frequency part is controlled by the stress parameter $\Delta\sigma$. The following assumption was used to obtain a realistic model describing spectra for the condition of VHR site. Every data set consisted of N spectra for earthquakes of magnitudes varying from M_{min} to M_{max}. Therefore, the spectrum for the "central" magnitude $M_C = (\Sigma M_i)/N$, representing ground acceleration for hard rock, should fit the mean values of empirical "average soil" spectra at low frequencies ($f < 0.1$-0.2 Hz), and it should generally be less than the mean empirical spectra at higher frequencies. It has been found that the acceleration spectra of most significant part of the records, starting from S-wave arrival, for very hard rock sites ($\rho = 2.8$ gm/cm^3, $\beta = 3.8$ km/sec) in the Taiwan area can be modeled accurately using the Brune ω-squared source model with magnitude-dependent stress parameter $\Delta\sigma$, that should be determined using recently proposed regional relationships between seismic moment (M_0) and magnitude (M_L) (Li and Chiu 1989)

$$\log_{10} M_0 = 19.043 + 0.914\, M_L \quad (7)$$

and between $\Delta\sigma$ and M_0 (Tsai 1997)

$$\log_{10} \Delta\sigma = -3.3976 + 0.02292 \log_{10} M_0 \pm 0.6177 \quad (8)$$

The kappa filter ($\kappa = 0.03$-0.04) may be used to modify the spectral shape.

The obtained source scaling and attenuation models allow a satisfactory prediction of the peak ground acceleration for rock and "average soil" soil sites, for magnitudes $4.5 \leq M \leq 6.5$ and distances up to about 200 km in the Taiwan region. Standard deviation of residuals between observed and calculated (using stochastic simulation) PGAs does not exceed 0.3 log unit.

PROCESSING OF THE DATA

Processing of the records consisted of visual inspection of every accelerogram, selection of the significant part of the record starting from S-wave arrival, and the computation of Fourier amplitude spectra of the horizontal components using a 10% cosine window. The spectra were smoothed using a three-point running Hanning average filter (twenty consecutive smoothings were applied for raw spectra to reveal gross features of site amplification).

Reference spectra were calculated using the model described above. Seismic moment (M_0) and stress parameter ($\Delta\sigma$) estimations are not available for almost all the earthquakes under consideration, therefore we used regional relationships (Equations 7 and 8) for preliminary evaluation of average values. Obviously, earthquake parameters that are necessary to the model of the spectrum for any given event may differ from those predicted from general models, due to peculiarities of the source-rupture process. At the same time, the possibility of an erroneous magnitude determination should also be taken into account. Therefore, for realistic estimates of VHR reference spectra, it is necessary to fit theoretical and empirical ones and to evaluate the proper earthquake source parameters to be used in the model. As a general statement for comparison, empirical and modeled spectra should be equal at low frequencies ($f < 0.1$-0.2 Hz) where influence of local conditions is believed to be negligible, and the fitting of the low-frequency part of the spectra allows us to evaluate a seismic moment. Ideally, recordings of every station should satisfy this condition, but the possible presence of long-period surface waves trapped within the basin may affect the low-frequency part of the spectra. The other source of uncertainty is the low signal-to-noise ratio (this problem will be discussed later).

The high-frequency part of the spectrum is controlled by stress parameter $\Delta\sigma$. When publishing his relation between stress parameter and seismic moment for northeastern Taiwan (Equation 8), Tsai (1997) noted that $\Delta\sigma$ values obtained in his study should be treated as upper-boundary values. When the proper value of seismic moment is evaluated, the estimation of stress parameters may be obtained assuming that the modeled spectrum (reference "very hard rock" site) should be generally less than empirical spectra at least for frequencies up to 10 Hz (Boore and Joyner 1997). Actually, a lot of "proper" values of the stress parameter may be accepted. However, as will be shown later, the procedure used in this approach is not sensitive to these uncertainties. If an earthquake has been registered at many stations, it is possible to compare source parameters evaluated for every station and to estimate the average values. In addition, this procedure also allows us to verify accepted source-scaling models. Figure 4 shows the comparison of source parameter estimations obtained by fitting modeled and empirical spectra for earthquakes considered in this study with those predicted using regional relationships.

It can be seen that individual estimations of earthquake source parameters to be used when calculating spectral ratios between empirical and modeled reference spectra are in good agreement with those predicted by regional relationships. However, seismic moment values estimated for shallow

earthquakes of magnitudes $M > 5.5$ (events 7, 15 and 27 in Table 2) are generally larger than regional averages. Most probably, long-period surface waves generated by distant shallow and relatively large earthquakes increase spectral amplitudes at low frequencies and result to overestimation of the seismic moment. For example, we used $M_0 = 9 \times 10^{25}$ dyne-cm for event 7 (M_L=6.2, H=5.3 km), while Ma and Kikuchi (1994) determined the seismic moment for this event using the long-period P-wave data to obtain a value of 3.75×10^{25} dyne-cm. However, this value is also higher than that expected using Equation 7 (5.2×10^{24} dyne-cm).

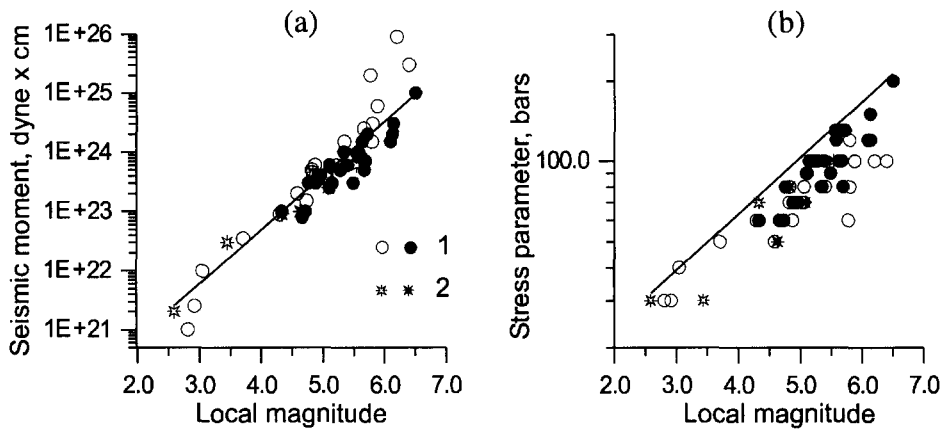

Figure 4. Comparison of the seismic moment (a) and stress parameter (b) estimations obtained by fitting the modeled and empirical spectra for the individual earthquakes. The solid lines represent regional source parameter/magnitude relationships; the symbols indicate the estimations for the individual shallow (open symbols) and deep (black symbols) earthquakes. 1= average values from several records, 2 = data from a single record.

The comparison of empirical spectra and modeled reference "very hard rock" spectra is shown in Figure 5. Station TAP53 is situated outside the Taipei basin (Figure 1) on a shallow layer of soft soil. Station TAP12 is situated in the center of the basin, and the thickness of Quaternary deposits in this part of the valley is about 200 meters. The empirical spectra reveal distinct amplification when compared with reference ones at frequencies of 4-6 Hz for station TAP53 and 1-3 Hz for station TAP12.

Because of the necessity to compare empirical and modeled spectra within a wide frequency range, it is necessary to estimate the uncertainty of the recorded spectra by determining signal-to-noise ratio. The observed signal may contain two types of noise: ambient seismic noise completely unrelated to the earthquake, and signal-generated noise (Field and Jacob 1995). In the used model, only ambient noise should be eliminated, because the second type of the noise (such as that produced by scattering) may be considered as a component of site response. Figure 6 shows the comparison between the signal window spectra and the pre-event noise spectra for records of two earthquakes: event 18 in Table 2 (M_L=6.5, H=40 km) and event 35 (M_L=3.7, H =8.6 km) obtained at station TAP99. As a rule, when computing the spectral ratios, only data with signal-to-noise ratio greater than 2-3 were used. It can be seen that the record of a small event does not satisfy this requirement for frequencies less than 0.8-0.6 Hz, and the low-frequency part of the record is affected by the ambient noise. In this case the signal-to-noise ratio allows us to analyze the spectra at frequencies from 0.8 Hz to 12-14 Hz. The shape of the signal spectra shows a distinct slope at frequencies less than 2 Hz until the spectra become affected by the ambient noise, and this feature has been used when estimating the frequency range to be analysed for every record.

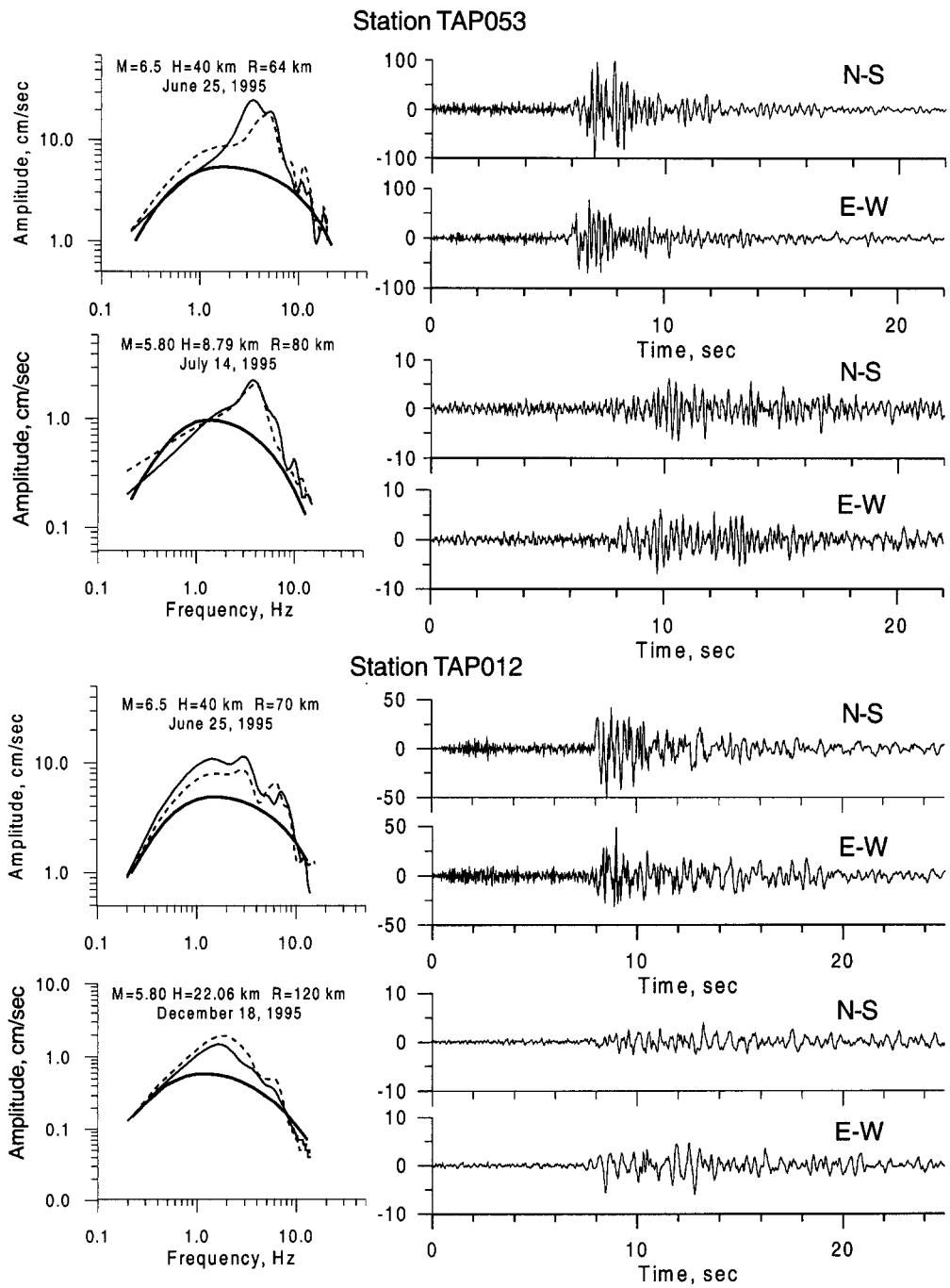

Figure 5. Comparison of the smoothed observed spectra (thin lines, solid lines = NS component, dashed lines = EW component) and reference "very hard rock" modeled spectra (thick lines) for earthquakes of magnitude M, hypocentral depth H, and hypocentral distance R.

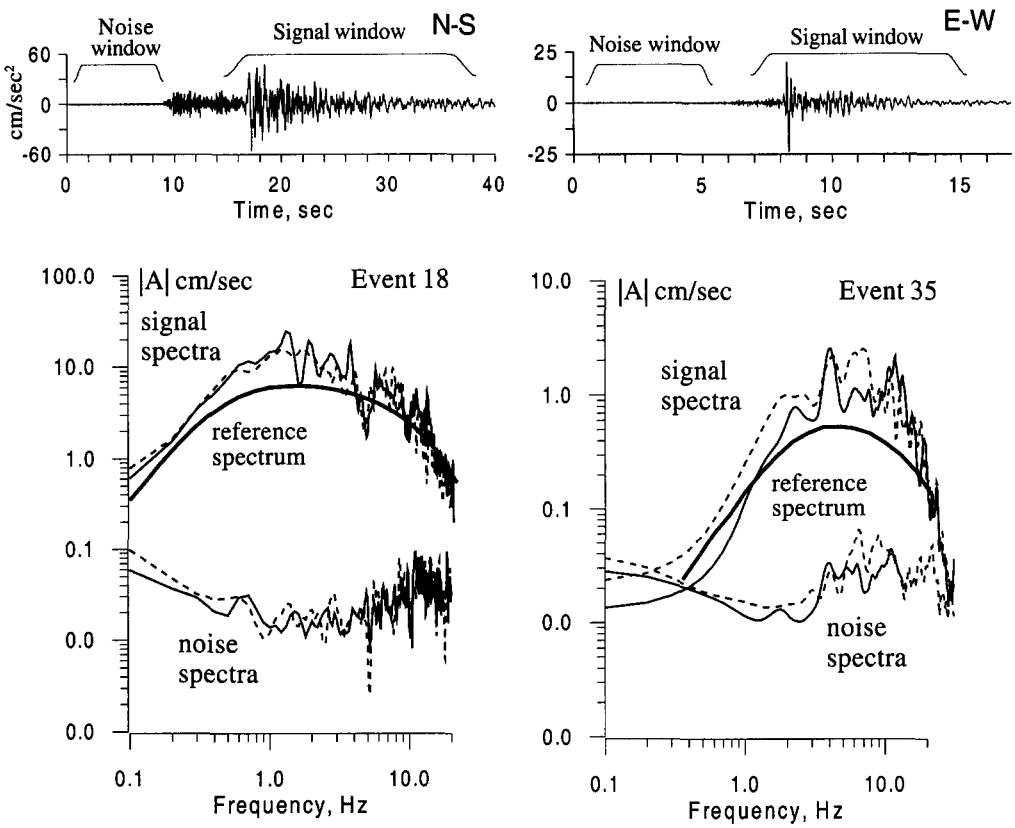

Figure 6. Signal and ambient noise spectra for a large distant earthquake (event 18, M=6.5, R= 65 km) and a small nearby earthquake (event 35, M=3.7, R=15 km) obtained at station TAP99. The thin lines represent spectra of the records (the solid lines = NS component, the dashed lines = EW component). The modeled reference "very hard rock" spectra are shown by thick, solid lines.

To minimize the uncertainties introduced by the choice of stress parameter to be used for reference spectra estimation, the spectral ratios were normalized assuming their maximum amplitude. Figure 7 shows the influence of accepted stress parameter values on an example of the record obtained at station TAP12 during an earthquake of M_L=5.8 (event 24 in Table 2). Even small variations in stress parameter could affect the amplitude of spectral ratios, but normalized ones are practically independent of the stress parameter value.

This approach, however, requires scaling of the normalized spectral ratios to estimate absolute amplitudes of the amplification. Generally, spectral ratios should approach unity at very low frequencies, and therefore the "basic value" of every SBSR function may be obtained by extrapolating its average curve to $f \sim 0.0$ Hz. On the other hand, theoretical modeling using available geotechnical information may be applied for scaling. However, it may introduce more uncertainty (Field and Jacob 1995).

RESULTS AND DISCUSSION

As previously explained, the spectral ratios for every record were calculated by dividing the actual spectra of horizontal components (A_H) by the modeled "very hard rock" spectrum (A_{VHR}). We

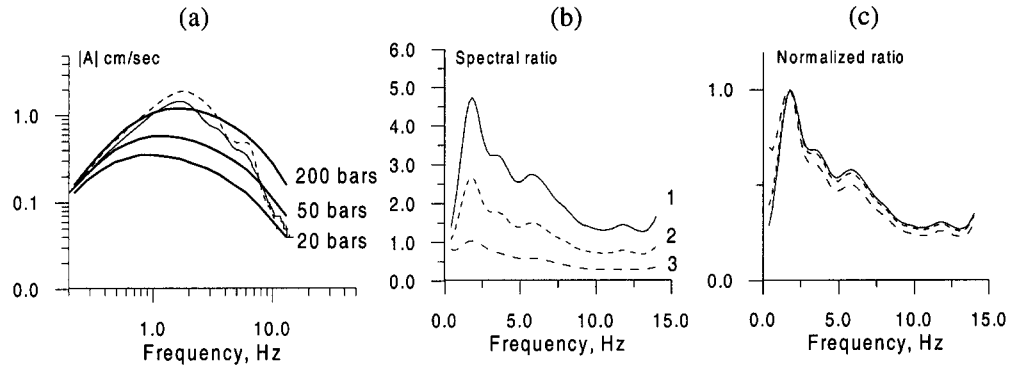

Figure 7. Influence of stress parameter value on spectral ratio estimation: (a) comparison of the smoothed record spectra (thin lines, the solid line = NS component, the dashed line = EW component, event 24 in Table 2) and the modeled reference "very hard rock" spectra (thick lines) for different stress parameter values; (b) spectral ratios obtained for NS-component using reference spectra with different stress parameter values: 1 - 20 bars; 2 - 50 bars, and 3 - 200 bars; (c) normalized spectral ratios.

determined the site amplification at the 35 stations. Initially, the characteristics of the site response were analysed regardless of the earthquake parameters. Figure 8 shows the statistical characteristics for a set of normalized site/bedrock spectral ratios (SBSR) calculated for stations situated near the deepest part of the Taipei basin (station TAP03), in the central part (station TAP12), near the edge (station TAP31), and outside the basin (station TAP53). Mean-amplification values ($SR_M = [\Sigma SR_i]/N$, shown by thick solid lines in Figure 8) reveal prominent peaks, and the amplitude and frequency of these peaks for stations situated within the basin depends both on the thickness of Quaternary deposits and the position of the station (see Figure 1). Station TAP53 is situated on a shallow layer of soft deposits outside the basin, and its SBSR curve shows a distinct amplification at frequencies around 4 Hz. The thin lines in Figure 8 from outer to inner represent ± 1 standard deviation and ± 1 standard deviation of the mean (standard error). The dashed lines in Figure 8 show the distribution of standard deviation versus frequency. It can be seen, for example, that the scatter of individual spectral ratios (represented by the standard deviation) decreases sharply within the frequency interval of maximum amplification for station TAP53. This ascertains that almost all earthquakes, regardless of magnitude, source depth and distance, produce an amplification at these frequencies (records from 14 deep and 8 shallow earthquakes were analysed for this station). Scatter distribution of the same character can be seen for station TAP31 and TAP03, and there are some peculiarities in the scatter for station TAP12. The first prominent peak of spectral amplification for station TAP12 is accompanied by a high standard deviation at frequencies of less than 3 Hz. The different character of the site-response characteristics during earthquakes of different depth and distances (Loh et al. 1998) may be considered as one of the possible sources of this increase in scatter.

The fact that the parameters of soil response may depend on the earthquake source depth shows the necessity to analyze spectral ratios for deep and shallow events separately. The database used in this study contains different numbers of recordings from deep and shallow events for every station. To represent the difference between site response during deep and shallow events in a satisfactory way, we analyzed the recordings of those stations that contain more than six records of deep and shallow earthquakes. It has been found that for several stations (TAP12, TAP13, TAP14, TAP15, TAP16, TAP32, TAP37 and TAP38) the difference is sufficient both at low and high frequencies (Figure 9), and may exceed a factor of 1.5 for mean amplification values. These stations are characterized by a shift of fundamental resonance peak to higher frequencies for deep earthquakes as compared with this

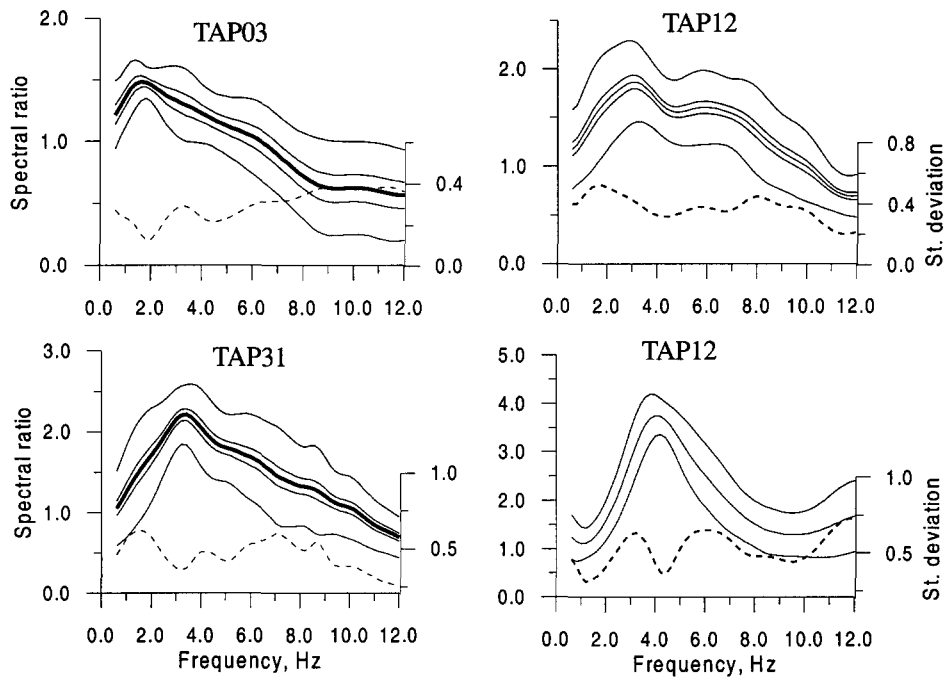

Figure 8. Characteristics of the site response functions. The thick solid lines represent mean-amplification values; the thin solid lines, from outer to inner, show ± 1 standard deviation and ± 1 standard deviation of the mean (standard error); the dotted lines represent standard deviation distribution versus frequency. Only ± 1 standard deviation limits are shown for station TAP53.

for shallow earthquakes. The detailed analysis of the two- and three-dimensional effect of wave propagation shows that the peaks of the transfer function of the local site effects can shift in their frequency and in amplitude with changing the angle of incidence, and the variation is a function of the narrow basin structure (e.g., Wong and Trifunac 1974, Bard and Bouchon 1985, Papageorgiou and Kim 1993, and Coutel and Mora 1998). On the other hand, it is necessary to study the possibility that the observed features of spectral amplification are caused by difference in the reference spectra modeled for distant deep and shallow earthquakes.

Actually, the only difference between the spectral models for deep and shallow earthquakes in the Taiwan region is the quality factor $Q(f)$ (Equation 4). A larger factor Q means a lower attenuation of the spectral amplitudes with distance. The shallow event model causes more rapid attenuation of the spectral energy at the high frequencies ($Q = 125f^{0.8}$) as compared with those for deep earthquakes ($Q = 225f^{1.1}$). To test the influence of the model parameter on the results of site response estimates, we processed the same data sets (the recordings obtained at some stations) using the different attenuation models (shallow and deep events) for all earthquakes. Figure 10 shows comparison of the amplification functions calculated for stations TAP15 and TAP22. These stations are located on the shallow Quaternary deposits in the eastern part of the valley, and station TAP15 reveals a shift of fundamental resonance peak to higher frequencies for deep earthquakes. It can be seen that the change of the model parameter (Q factor) does not affect the character of site response functions for deep and shallow earthquakes. At the same time, the use of proper models results in the least scatter of the data in the vicinity of fundamental resonance peak (Figure 11). It is reasonable to assume that the observed difference in the site response for deep and shallow earthquakes is an intrinsic feature of the sites, and it is caused by a combination of site, source, and propagation path effects.

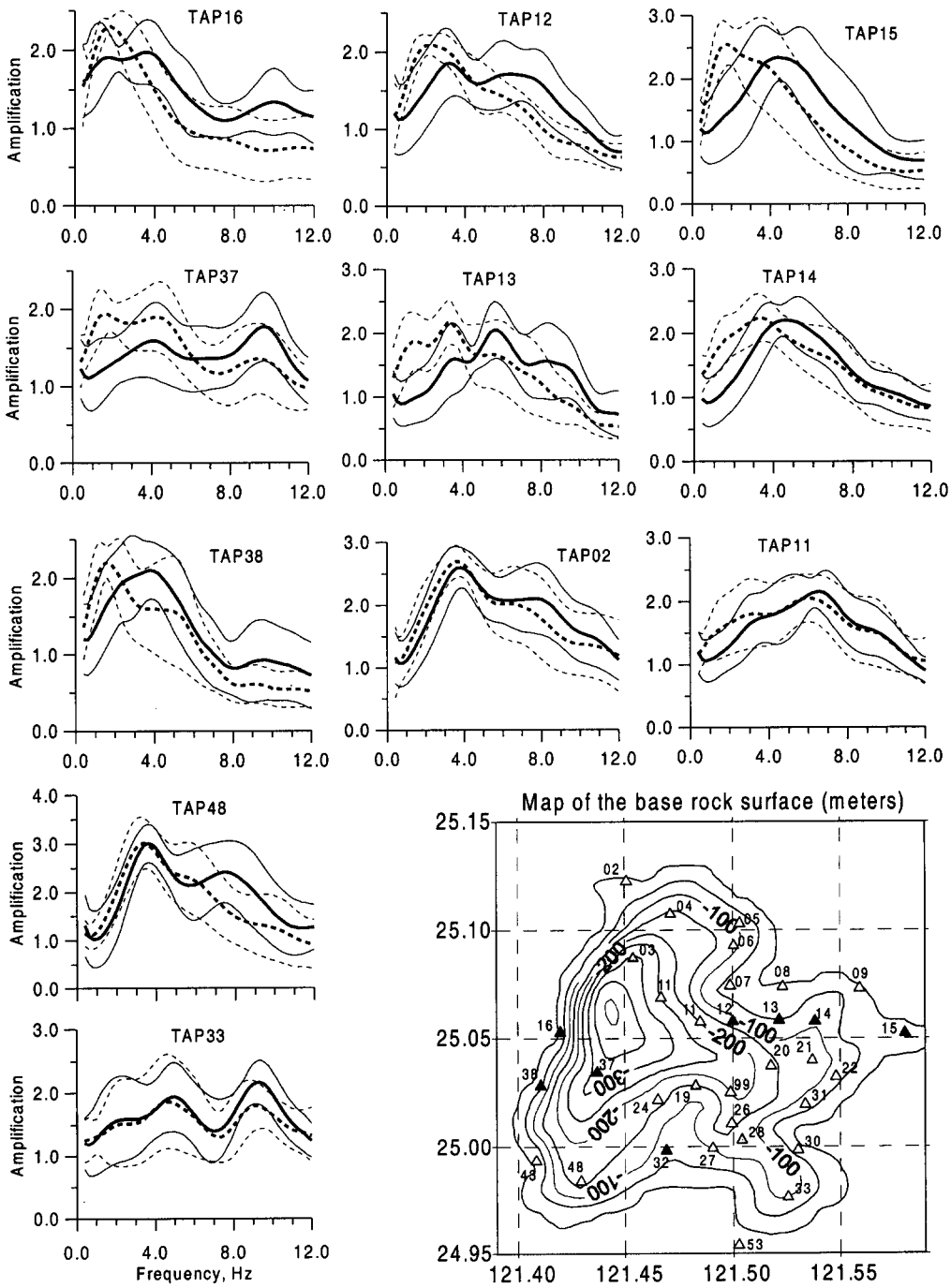

Figure 9. Comparison of the site-response characteristics that were determined for deep (solid lines) and shallow (dashed lines) earthquakes. The thick lines represent mean-amplification values; the thin lines show ± 1 standard deviation limits. The black triangles on the map indicate the stations showing the shift of the fundamental frequency of site response to higher frequencies for deep events; the white triangles indicate the stations revealing no prominient difference; the gray triangles indicate the stations with no sufficient data to study the amplification functions for deep and shallow events separately.

Depending on the shape of the mean-amplitude spectral ratios, the sites may be divided into three categories: 1 — sites that are characterized by a single prominent peak for the amplification within a relatively narrow frequency band; 2 — multiple, but well-defined, resonances (stations TAP09, TAP21, TAP26, TAP29, TAP30, TAP33, TAP54, TAP99); 3 — broadband amplification (stations TAP05, TAP08, TAP10, TAP11, TAP24, TAP032, TAP037, TAP043). The first category, in turn, may be divided into two subcategories: 1a — the fundamental response frequency does not depend on the earthquake depth (e.g. stations TAP02, TAP03, TAP06, TAP20, TAP22, TAP27, TAP48, TAP53) and 1b — the resonance frequencies are different for deep and shallow events (TAP12, TAP13, TAP14, TAP15, TAP16, TAP38). On the one hand, it is possible to conclude that the type of amplification relates to the site geology. Resonance at a single frequency occurs when there is a uniform well-defined layer over bedrock, and the influence of other layers is negligible. Multiple resonances are caused by a small number of well-defined layers, and broadband amplification may occur when there is a gradual increase of shear-wave velocity with the depth. On the other hand, uneven basement topography and complex local structure may also produce additional resonance peaks and be a source of considerable variability in the spectral ratios.

When analyzing the spectral ratios with a single prominent peak, it can be seen that the frequency of the peak reveals a tendency to shift between sites as the depth to the bedrock changes. Station TAP03, situated near the deepest part of the basin, shows a peak of amplification at a frequency of about 1.0 Hz (Figure 8), while station TAP22, located near the basin edge on shallow (thickness less than 50 meters) Quaternary deposits, is characterized by the largest amplification at frequencies 4.5-5.0 Hz (Figure 10). To verify the ability of the applied method to represent the amplitude and frequency dependence of site response, we used a simple 1-D technique that allows us to calculate the theoretical spectral amplification of a multilayer soil column overlying the rigid halfspace for SH- and SV-waves approaching the bottom of the soil with arbitrary angles of incidence. When constructing the typical models of soil columns (Table 3), we used the values of shear-wave velocities V_S listed in Table 1, the values of density ρ are assumed to be 1.6 gm/cm^3 for the top layer of Sungshan formation, 2.0 gm/cm^3 for the basement, and gradually increasing values of density (from 1.7 gm/cm^3 to 1.95 gm/cm^3) were assigned to other formations of Quaternary deposits. The quality factor $Q(f)$ that represents the damping in the soil was taken as follows (Wen and Peng 1998b): Sungshan formation, top layer, $Q(f) = 3.6f^{0.96}$; second layer, $Q(f) = 5.6f^{0.99}$; bottom layer, $Q(f) = 7.0f^{0.99}$; Chingmei formation, $Q(f) = 10.2f^{1.1}$; Wuku and Panchiao formations, $Q(f) = 40f^{1.1}$. A very low Q value is expected for high-crack density and fluid-saturated soil in the Taiwan area (Shien 1992), therefore these values, which were accepted for the calculations, are not suprising. However, it is necessary to note that the geotechnical properties of the Quaternary deposits in the Taipei basin have still not been studied in detail.

Theoretical spectral ratios were calculated for horizontal components of motion for SH- and SV-waves using different angles of incidence. Actually, the angles for different S-wave portions may vary significantly depending on the peculiarities of the earthquake source and propagation path. Figure 12 shows a comparison between theoretical spectral ratios that were obtained using 1-D models (average values for SH- and SV-waves and for six incidence angles: 10^0, 20^0, 30^0, 40^0, 50^0, and 60^0) and empirical ratios for stations that are characterized by different thickness of Quaternary deposits and approximately the same character of the site response during deep and shallow earthquakes. It is seen that multilayered models reveal good agreement with empirical data, and the theoretical curves lay within ± 1 standard deviation limits. Amplitudes on the amplification peaks depend on the impedance ratio between the basement ($V_{S1}\rho_1$) and layer ($V_{S2}\rho_2$), and the quality factor $Q(f)$ combined with the layer thickness determines the amplification at high frequencies. Most probably, the difference between amplitudes of theoretical and empirical spectral ratios is caused by discrepancy in accepted and real properties of the Quaternary deposits.

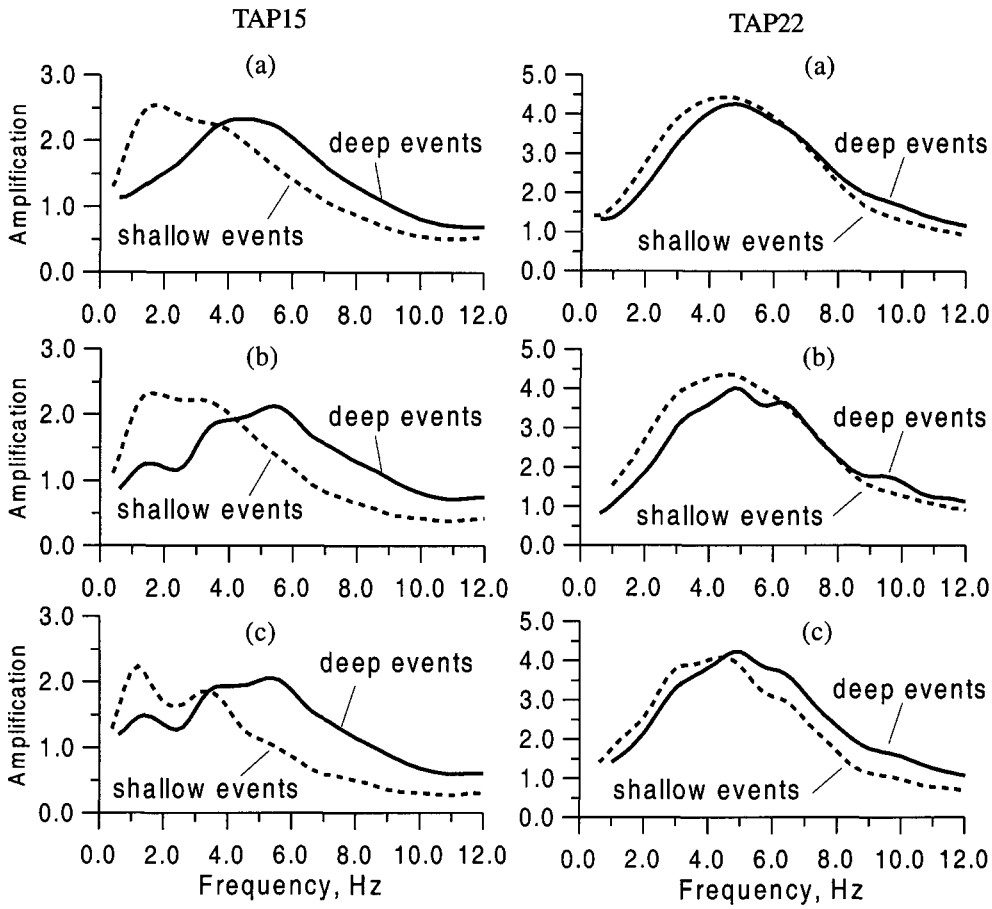

Figure 10. Comparison of spectral ratios (mean amplification values) that were calculated using the proper attenuation models for shallow and deep events (a); the shallow-earthquake attenuation model was used for all events (b); the deep-earthquake attenuation model was used for all events (c).

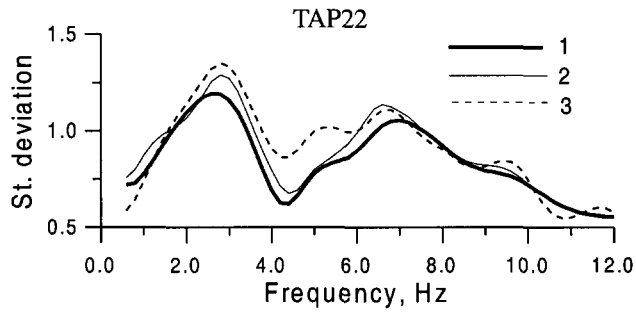

Figure 11. Comparison of the standard deviation of spectral ratios calculated for station TAP22 using different attenuation models. The proper attenuation models were used for shallow and deep events (1); the deep-earthquake attenuation model was used for all events (2); the shallow-earthquake attenuation model was used for all events (3).

Table 3. Parameters of the soil column models

Formation	Vp (km/sec)	Vs (km/sec)	Density, gm/cm^3	Thickness, km
TAP03				
Sungshan	1.5	0.25	1.6	0.02
	1.6	0.34	1.7	0.06
Chingmei	1.8	0.5	1.8	0.04
Wuku	2.0	0.6	1.9	0.08
Basement	3.0	1.2	2.0	—
TAP10				
Sungshan	0.45	0.17	1.6	0.01
	1.6	0.34	1.65	0.02
			1.7	0.04
Chingmei	1.8	0.5	1.8	0.05
Wuku	2.0	0.6	1.9	0.08
Basement	3.0	1.2	2.0	—
TAP99				
Sungshan	1.5	0.25	1.6	0.01
	1.6	0.34	1.7	0.02
Chingmei	1.8	0.5	1.8	0.03
Wuku	2.0	0.6	1.9	0.08
Basement	3.0	1.2	2.0	—
TAP24				
Sungshan	1.5	0.25	1.6	0.01
	1.6	0.34	1.7	0.02
Chingmei	1.8	0.5	1.8	0.04
Wuku	2.0	0.6	1.9	0.04
Basement	3.0	1.2	2.0	—
TAP27				
Sungshan	1.6	0.34	1.7	0.01
Chingmei	1.8	0.5	1.8	0.02
Wuku	2.0	0.6	1.9	0.04
Basement	3.0	1.2	2.0	—
TAP29				
Sungshan	1.5	0.25	1.6	0.025
Chingmei	1.8	0.5	1.8	0.01
Basement	3.0	1.2	2.0	—
TAP07				
Sungshan	1.6	0.3	1.7	0.02
Chingmei	1.8	0.5	1.8	0.02
Basement	3.0	1.2	2.0	—
TAP31				
Sungshan	1.5	0.25	1.6	0.01
Chingmei	1.8	0.5	1.8	0.02
Basement	3.0	1.2	2.0	—

At the same time, the 1-D model fails to predict site amplification for station TAP10 located in the deep part of the Taipei basin. Empirical spectral ratios for this station and station TAP11 show "a lack" of low-frequency amplification and relatively high amplitudes at moderate frequencies as compared with the nearest stations, which are characterized by approximately the same thickness of sediments (e.g., TAP03). A detailed map of the basement depth (Lee et al. 1978; see Figure 1) shows narrow crests across the valley in its southern and northern parts. It is reasonable to suppose, that the influence of these crests (scattering of the seismic waves on the basement irregularities) is a source of the above-mentioned peculiarities in site response for stations situated near the crest slopes. These effects are more pronounced in the central part of the basin where the changes in basement topography are the steepest and the stations are located on the "lee side," meaning the direction from which seismic waves are propagated. The 3-D modeling is necessary to verify these suggestions.

Since the Taipei basin may be considered a wide, shallow alluvial valley (depth/length ratio less than 0.25), it is interesting to study the so-called basin effect — the peculiarities of the response should depend on the site location relatively the basin edge. The sediment-basement rock interface may generate vertically propagating shear waves from the edges. Therefore, as has been shown recently (e.g., Bard and Gariel 1986, Silva 1989, and Jongmans and Campillo 1990), the 1-D model may be inadequate at high frequencies near the edge of the sediments. In the case of the Taipei valley, the site response for the stations that are located near the basin edges may be classified as a single or multiple resonances (e.g., stations TAP31 and TAP29, Figure 12), and it may be described by the influence of an uniform soft layer or a small number of well-defined layers over bedrock. For station TAP29, for example, the amplification peak at frequency of about 2 Hz is caused by response of a soft (V_S=200-300 m/sec, thickness 25-35 meters) layer of Shungshan formation, and a relatively rigid (V_S=500-600 m/sec) and thin (thickness of about 10 meters) layer of Chingmei formation causes the amplification at a frequency of about 7 Hz. However, the site response for stations TAP29 and TAP30 is also characterized by prominent amplification at frequencies of more than 10 Hz, which could not be explained by a simple 1-D model. It is necessary to note that these stations are located near an irregularity of the basin edge (see Figure 1). In general, it is possible to conclude that, for most stations, there is no clear evidence of the "basin-edge effect," at least at frequencies up to 10-12 Hz, and the 1-D model can be used for calculation of the site amplification in the Taipei basin at frequencies of from 0.4-0.5 to 10-12 Hz.

Figure 13 shows the distribution of the frequency of the maximum amplification (fundamental resonance) peaks for shallow earthquakes. It can be seen that, except for the northwestern part of the basin, there is no correlation between the frequency of the peak amplification and the thickness of the whole Quaternary deposits or Sungshan formation. The central part of the Taipei basin reveals maximum amplification at frequencies of more than 3-4 Hz, the northwestern and southeastern parts show the relatively low-frequency (less than 2-3 Hz) amplification. It seems reasonable to suppose that the site amplification in the central part of the basin is determined by the properties of multilayered deposits and by the influence of basement topography. Near the edges of the basin, the frequency of peak amplification depends on the local peculiarities of the relatively shallow soil layers. It is necessary to note that the frequencies of peak amplification do not necessarily represent so-called dominant frequencies of the ground motion, which depend on the source, path, and site effect. However, the schemes of fundamental resonance frequencies should be useful when determining the type of construction (natural frequency) to be erected.

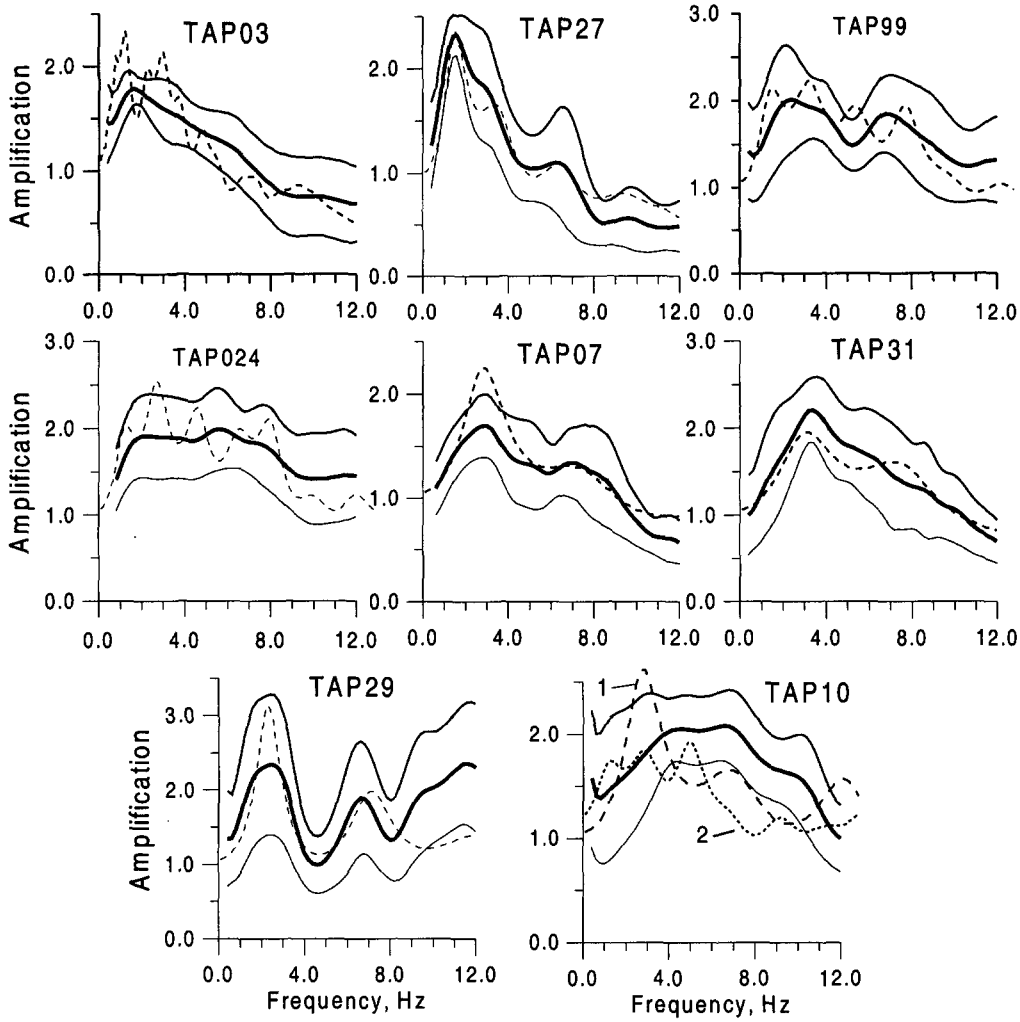

Figure 12. Comparison between the empirical spectral ratios (solid lines; the thick line shows mean-amplitude values and the thin lines show ± 1 standard deviation limits) and theoretical spectral ratios (dashed lines, the average curve for SH- and SV-waves), which were calculated using 1-D models. Theoretical spectral ratios for station TAP10: 1 = the model that describes the whole Quaternary deposits (5 layers); 2 = the model that describes the upper Sungshan formation (3 layers).

CONCLUSION

In this study we used a modification of the spectral ratio method based on the calculation of frequency response at each station with respect to a hypothetical "very hard rock"(VHR) site. The method allows us to estimate site amplifications from all the recordings even though there is no reference rock station available. The reference VHR spectra are obtained using source scaling and attenuation models recently established for Taiwan region. This approach also allows us both to estimate the influence of source and propagation path effects on the site response and, when using large enough numbers of earthquakes, to evaluate the variability of spectral ratios that is important for probabilistic assessment of seismic hazard.

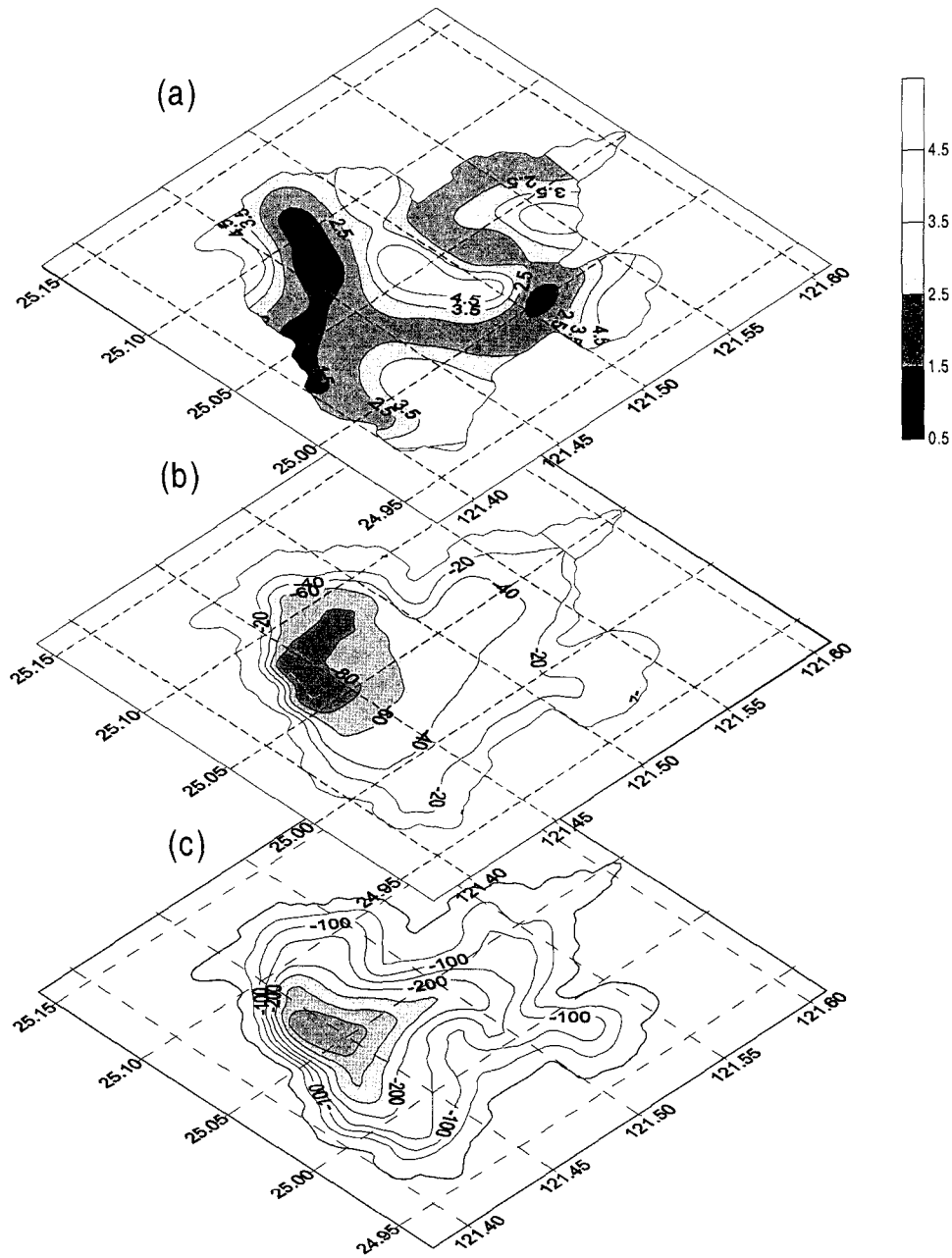

Figure 13. (a) Distribution of the frequency (Hz) of maximum amplification (fundamental resonance) along the Taipei basin, shallow earthquakes; (b) Map of the bottom (meters) of Sungshan formation; (c) Map of the thickness (meters) of Quaternary deposits along the Taipei basin.

Recordings from 66 earthquakes obtained at 35 stations in the TSMIP network in the Taipei area were used in this study. The magnitude range was from 2.6 to 6.5 on the local magnitude scale, focal depth was between 1 km and 118 km, and the hypocentral distance range was from 10-15 km to 150-160 km. Horizontal-component site-amplification data were obtained within the frequency interval 0.4 Hz to 12 Hz. The ensemble averages of the site-response estimation are consistent with theoretical modeling of the amplification curves both in amplitude, resonance frequencies, and overall shape. The conclusions may be summarized as follows:

1. The method of S-wave site-response estimation relative to a regional spectral model for hypothetical "very hard rock" site has been found capable of providing the reliable estinations of site amplification at locations where a nearby reference site is not available. The use of the method to analyse the recordings of the TSMIP network provides us with an opportunity to study the peculiarities of the site response in the Taipei sedimentary basin. The results in conjunction with "very hard rock" spectral model will be used for "site-dependent" seismic hazard assessment.

2. The spectral characteristics of the site response in the Taipei basin show that the frequency of maximum amplification peak (fundamental resonance) does not necessarily depend on the thickness of Quaternary deposits that fill the valley. The site amplification is determined by the properties of multilayered and complex structure of the deposits and the valley configuration.

3. The amplitude and shape of spectral ratios may be different for deep and shallow events. In this case, the site-response characteristics for shallow events, in general, show relatively low-frequency amplification, while those for deep events also reveal prominent peaks in the high-frequency domain. The difference between averaged spectral ratios for shallow and deep earthquakes may exceed a factor of 1.5 at certain frequencies, however, their ± 1 standard deviation limits overlap each other.

4. The site response for stations located near the edge of the basin can be modeled accurately by a 1-D model using a few shallow low-impedance surface layers. A complex multilayer 1-D model is required to describe the site amplification for the stations located on the deep sediments. However, the 1-D models fail to predict spectral ratios for the sites located near subsurface topographic irregularities.

Of course, there are some unresolved problems. To validate the proposed method, we used one-dimensional models whose parameters were estimated independently. To check the results thoroughly, it seems to be useful also to use the other nonreference-site-dependent techniques such as the inversion scheme introduced by Boatwright et al. (1991), as well as the 2-D and 3-D modeling. The comparison of the predicted and empirical strong motion data should also allows to verify the model. As can be seen from Figure 3, the local site response in the Taipei basin, except for a few small earthquakes that are located directly under the basin, was studied using the records from earthquakes that occurred from 1993 to 1998 and located to the southeast of the basin. The influence of azimuthal direction of incident excitation on the response of the Taipei basin should be studied on the basis of the data obtained recently during the strong Chi-Chi earthquake of September 21, 1999 (M_L=7.3) and its aftershocks. These earthquakes occurred to the south and southwest of the basin (in the center of Taiwan island), and provide a unique set of TSMIP recordings.

In this paper we do not consider peculiarities of the site response with respect to the direction of the records components. This analysis, as well as the detailed study of the spectral ratio varia-bility with respect to the earthquake source depth, requires inclusion of more earthquake recordings from the stations under consideration and for collection of the data from other stations located within (and in the vicinity) of the Taipei basin. At the same time it is necessary to study the site response in the low frequency (below 1 Hz) domain. These are topics for future research.

ACKNOWLEDGMENTS

The authors are very grateful to anonymous reviwers for their comments and suggestions for improving the manuscript. This study was carried out in the National Center for Research on Earthquake Engineering and was supported by the National Science Council under the grant NSC87-2621-P-319-001.

REFERENCES

Akamatsu, J., Onoue, K., Morikawa, H., Nishimura, K., Nakamura, M., Seto., N., Komazawa, M., Jiang, L., Li, K., Luo, Q., and Wang, Y., 1998, Bedrock structure in Lijiang basin and its seismic effect, *Proc. of the Second Int. Symp. on the Effects of Surface Geology on Seismic Motion,* Yokohama, Japan, 1-3 December, 1998, Balkema, Rotterdam, 725-732.

Aki, K., 1988, Local site effect on strong ground motion, *Recent Advances in Ground-Moyion Evaluation, Proc. Earthquake Eng. Soil Dyn.*, **II**, J. L. Von Thun (Editor), Geotechnical Special Publication No. 20, Am. Soc. Civ. Engr., New York, 103-155.

Anderson, J. and Hough, S., 1984, A model for the shape of the Fourier amplitude spectrum of acceleration at high frequencies, *Bull. Seism. Soc. Am*, **74**, 1969-1993.

Andrews, D. J., 1986, Objective determination of source parameters and similarity of earthquakes of different size, *Earthquake Source Mechanics,* S. Das, J. Boatwright, and C. H. Sholtz (Editors), American Geophysical Union, Washington, D.C.

Bard., P. Y. and Bouchon, M., 1985, Two-dimensional resonance of sediment-filled valleys, *Bull. Seism. Soc. Am.*, **75**, 519-541.

Bard, P. Y. and Gariel, J. C., 1986, The seismic response of two-dimensional sedimentary deposits with large vertical velocity gradients, *Bull. Seism. Soc. Am.*, **76**, 343-366.

Bard, P. Y., 1995, Effects of surface geology on ground motion: recent results and remaining issues, *Proc. of 10th European Conference on Earthquake Engineering*, Balkema, Rotterdam, 305-323.

Boatwright, J., Fletcher, J. B., and Fumal, T. E., 1991, A general inversion scheme for source, site and propagation characteristics using multiply recorded sets of moderate-sized earthquakes, *Bull. Seism. Soc. Am.*, **81**, 1754-1782.

Boore, D. M., 1983, Stochastic simulation of high frequency ground motion based on seismological model of the radiated spectra, *Bul. Seism. Soc. Am.*, **73**, 1865-1894.

Boore, D. M. and Joyner, W. B., 1997, Site amplifications for generic rock sites, *Bull. Seism. Soc. Am*, **87**, 327-341.

Bonilla, L. F., Steidl, J. H., Lindley, G. T., Tumarkin, A. G., and Archuleta, R. J., 1997, Site amplification in the San Fernando Valley, California: variability on site-effect estimation using the S-wave, coda, and H/V methods, *Bull. Seism. Soc. Am.*, **87**, 710-730.

Borcherdt, R. D., 1970, Effect of local geology on ground motion near San Francisco Bay, *Bull. Seism. Soc. Am.*, **60**, 29-61.

Borcherdt, R. D., Glassmoyer, G., Der Kiurghian, A., and Cranswick, E., 1989, Results and data from seismologic and geologic studies following earthquakes of December 7, 1988 near Spitak, Armenia, SSSR, *U.S. Geol. Surv. Open-File Rep.*, 89-136A.

Brune, J. N., 1970, Tectonic stress and the spectra of seismic shear waves from earthquakes, *J. Geophys. Res.*, **75**, 4997-5009.

Campillo, M., Bard, P. Y., Nicollin, F., and Sanchez-Sesma, F., 1988, The incident wavefield in Mexico City during the Great Michoacan Earthquake and its interaction with the deep basin, *Earthquake Spectra*, **4**, 591-608.

Cassidy, J. F., Rogers, G. C., and Weicherd, D. H., 1997, Soil response on the Fraser Delta to the M_W=5.1 Duvall, Washington, earthquake, *Bull. Seism. Soc. Am.*, **87**, 1354-1361.

Chavez-Garcia, F. J., Ramos-Martinez, J., and Romero-Jimenez, E., 1995, Surface-wave dispersion analysis in Mexico City, *Bull. Seism. Soc. Am.*, **88**, 30-42.

Coutel, F. and Mora, P., 1998, Simulation-based comparison of four site-response estimation techniques, *Bull. Seism. Soc. Am.*, **82**, 81-103.

Fei, L. Y. and Lai, T. C., 1994, The preliminary result of an integrated survey of subsurface geology and engineering environment of the Taipei basin, *Proc. of the Joint Symp. on Taiwan Quaternary (5) and on Investigation of Subsurface Geology/Engineering Environment of Taipei Basin*, 121-128.

Field, E. H., 1996, Spectral amplification in a sediment filled valley exhibiting clear basin-edge-induced waves, *Bull. Seism. Soc. Am.*, **86**, 991-1005.

Field, E. H. and Jacob, K. H., 1995, A comparison and test of various site-response estimation techniques, including three that are not reference-site dependent, *Bull. Seism. Soc. Am.*, **85**, 1127-1143.

Graves, R. W., 1998, Three-dimensional computer simulations of realistic earthquake ground motions in regions of deep sedimentary basins, *Proc. of the Second Int. Symp. on the Effects of Surface Geology on Seismic Motion*, Yokohama, Japan, 1-3 December 1998, Balkema, Rotterdam, 103-120.

Graves, R. W. and Clayton, R. W., 1992, Modeling path effects in three-dimensional basin structures, *Bull. Seism. Soc. Am.*, **82**, 81-103.

Graves, R. W., Pitarka, A., and Somerville, P. G., 1998, Ground-motion amplification in the Santa Monica area: effects of shallow basin-edge structure, *Bull. Seism. Soc. Am.*, **88**, 1224-1242.

Hanks, C. and Brady, A. G.., 1991, The Loma prieta earthquake, ground motion and damage in Oakland, Treasure Island, and San Francisco, *Bull. Seism. Soc. Am.*, **81**, 2019-2047.

Hisada, Y., Aki, K., and Teng, T.-L., 1993, 3-D simulation of surface wave propagation in the Kanto sedimentary basin, Japan. Part 2: application of the surface wave BEM, *Bull. Seism. Soc. Am.*, **31**, 1700-1720.

Irikura, K., Iwata, T., Sekiguchi, H., and Pitarka, A., 1996, Lessons from the 1995 Hyogo-Ken Nanbu earthquake: why were such destructive motions generated to buildings? *J. of Nat. Dis. Sci.*, **17**, 99-127.

Jongmans, D., Pitilakis, K., Demanet, D., Raptakis, D., Riepl, J., Horrent, C., Tsokas, G., Lontzetidis, K., and Bard., P. Y., 1988, EURO-SEISTEST: determination of the geological structure of the Volvi basin and validation of the basin response, *Bull. Seism. Soc. Am.*, **88**, 473-487.

King, J. L. and Tucker, B. E., 1984, Observed variations of earthquake motion across a sediment-filled valley, *Bull. Seism. Soc. Am.*, **74**, 137-151.

Kudo, K., 1994, Practical estimates of site response, *Proc. V Conf. on Seismic Zonation*, Nice, 1878-1907

Kuo, K. W., Shin, T. C., and Wen, K. L., 1995, Taiwan strong motion instrumentation program (TSMIP) and preliminary analysis of site effects in Taipei basin from strong motion data, *Urban disaster mitigation: the Role of Engineering and Technology*, F. Y. Cheng and M. S. Cheu (Editors), Elsevier Science Ltd, 47-62.

Lachet, C. D., Hatzfeld, D., Bard, P. Y., Theodulidis, N., Papaioannou, C., and Savvadis, A., 1996, Site effect and microzonation in the city of Thessaloniki (Greece): comparison of different approaches, *Bull. Seism. Soc. Am.*, **86**, 1692-1703.

Lee, V. W., 1984, Three-dimensional diffraction of plane P, SV and SH waves by a hemispheric alluvial valley, *J. Soil Dyn. Earthquake Eng.*, **3**, 133-144.

Lee, C. M., W., Cheng, Y. M., and Wang, Y., 1978, Geology of the Taipei basin, *Taiwan Mining*, **30**, 350-380 (in Chinese)

Lermo, J. and Chavez-Garcia, F. J., 1993, Site effect evaluation using spectral ratios with only one station, *Bull. Seism. Soc. Am.*, **83**, 1574-1594.

Li, C. and Chiu, H. C., 1989, A simple method to estimate the seismic moment from seismograms, *Proc. Geol. Soc. China*, **32**, 197-207.

Loh, C. H., Hwang, J. Y., and Shin, T. C., 1998, Observed variation of earthquake motion across a basin – Taipei city, *Earthquake Spectra*, **14**, 115-133.

Ma, K. F. and Kikuchi, M., 1994, Initial investigation of the May 24, 1994 Hualen and June 5, 1994 Nanao earthquakes, *Terr. Atm. Oce.*, **5**, 611-623.

Papageorgiou, A. S. and Kim, J., 1991, Study of the propagation and amplification of seismic waves in Caracas Valley with reference to the 29 July 1969 earthquake: SH waves, *Bull. Seism. Soc. Am.*, **81**, 2214-2233.

Papageorgiou, A. S. and Kim, J., 1993, Propagation and amplification of seismic waves in 2-D valleys excited by obliquely incident P- and SV-waves, *J. of Earthquake Engineering and Structural Dynamics,* **22**, 428-440.

Pitarka, A., Irikura, K., Iwata, T., and Sekiguchi, H., 1998, Three dimensional simulation of the near fault ground motion for the 1995 Hyogo-Ken Nanbu (Kobe), Japan, Earthquake, *Bull. Seism. Soc. Am.*, **88**, 428-440.

Riepl, J., Bard, P. Y., Hatzfeld, D., Papaioannou, C., and Nechtschen, S., 1998, Detailed evaluation of site-response estimation methods across and along sedimentary valley of Volvi (EURO-SEISTEST), *Bull. Seism. Soc. Am.*, **88**, 488-502.

Rodriguez-Zuniga, J. L., Sanchez-Sesma, F. J., and Perez-Rocha, L. E., 1995, Seismic response of shallow alluvial valleys: the use of simplified models, *Bull. Seism. Soc. Am.*, **85**, 890-899.

Sanchez-Sesma, F. J., Chavez-Garcia F. J., and Bravo, M. A., 1988, Seismic response of a class of alluvial valleys for incident SH waves, *Bull. Seism. Soc. Am.*, **78**, 83-95.

Seed, H. B., Romo, M. R., Sun, J., Jame, A., and Lysmer, J., 1987, Relationships between soil conditions and earthquake ground motions in Mexico City in the earthquake of September 19, 1985, *Report UCB/EERC 87/15*, Earthquake Engineering Research Center, University of California, Berkeley.

Shieh, C.-F., 1992, Estimation of Q value by SP/S spectral ratio, *Terr. Atm. Oce.*, **3**, 469-482.

Silva, W. J., 1989, Site geometry and global characteristics, state-of-art report. *Proc. of Workshop on Dynamic Soil Properties and Site Characterization*, National Science Foundation and Electric Power Research Institute, Palo Alto, CA.

Sokolov, V. Yu., 1997, Empirical models for estimating Fourier-amplitude spectra of ground acceleration in the northern Caucasus (Racha seismogenic zone), *Bull. Seism. Soc. Am.*, **87**, 1401-1412.

Sokolov, V. Yu., 1998a, Rough estimation of site response using earthquake ground motion records, *Proc. of the Second Int. Symp. on the Effects of Surface Geology on Seismic Motion,* Yokohama, Japan, 1-3 December, 1998, Balkema, Rotterdam, 517-522.

Sokolov, V. Yu., 1998b, Spectral parameters of the ground motion in Caucasian seismogenic zones, *Bull. Seism. Soc. Am.*, **88**, 1438-1444.

Sokolov, V. Yu., Loh, C. H., and Wen K. L., 1999, Empirical models for estimating design input ground motions in Taiwan region, *Proc. of International Workshop on Mitigation of Seismic Effects on Transporation Structures,* Taipei, Taiwan, July 12-14, 1999, 154-163.

Sokolov, V. Yu., Loh, C. H., and Wen, K. L., 2000, Empirical model for estimating Fourier amplitude spectra of ground acceleration in Taiwan region, *J. of Earthquake Engineering and Structural Dynamics*, **29**, 339-357.

Somerville, P., 1998, Ground motion attenuation relationships and their application to aseismic design and seismic zonation, *Proc. of the Second Int. Symp. on the Effects of Surface Geology on Seismic Motion*, Yokohama, Japan, 1-3 December 1998, Balkema, Rotterdam, 35-49.

Stewart, S. P., Bray, J. D., Seed. H. B., and Sitar, N., 1994, Preliminary report on the principal geotechnical aspects of the January 17, 1994 Northridge earthquake, Earthquake Engineering Research Center *Report No USB/EERC 94-08*, University of California, Berkeley.

Su, F., Anderson, J. G., and Zeng, Y., 1998, Study of weak and strong ground motion including nonlinearity from the Northridge, California, earthquake sequence, *Bull. Seism. Soc. Am.*, **88**, 1411-1425

Tsai, C-C. P., 1997, Relationships of seismic source scaling in the Taiwan region, *Terr. Atm. Oce.*, **8**, 49-68.

Tucker, B. E. and King, J. L., 1984, Dependence of sediment-filled valley response on input amplitude and valley properties, *Bull. Seism. Soc. Am.*, **74**, 153-165.

Uetake, H. and Satoh, T., 1998, Recent array experiments in Japan, *Proc. of the Second Int. Symp. on the Effects of Surface Geology on Seismic Motion*, Yokohama, Japan, 1-3 December 1998, Balkema, Rotterdam, 51-70.

Wang, C. Y., Hsiao, W. C., and Sun, T. C., 1994, Reflection seismic stratigraphy in the Taipei basin (I) — Northestern Taipei, *J. Geol. Soc. China*, **37**, 69-95.

Wang, C. Y., Lee, Y. H., and Chang, H. C., 1996, P- and S-wave velocity structures of the Taipei basin, *Symposium on Taiwan strong motion instrumental program (II)*, Central Weather Bureau, 171-177.

Wang, J. H., 1993, Q values of Taiwan: a review, *J. Geol. Soc. of China*, **36**, 15-24.

Wang-Lee, C. M. and Lin, T. P., 1987, The geology and land subsidence of the Taipei basin, *Memoir Geol. Soc. China*, **9**, 447-467.

Wen, K. L., Peng, H. Y., Liu, L. F., and Shin, T. C., 1995, Basin effect analysis from a dense strong motion observation network, *Earthq. Eng. Struct. Dyn.*, **24**, 1069-1083.

Wen, K. L. and Peng, H.-Y., 1998a, Site effect analysis in the Taipei basin: results from TSMIP network data. *Terr. Atm. Oce.*, **9**, 691-704.

Wen, K. L. and Peng, H. Y., 1998b, Strong ground motion observations in the Taipei basin, *Proc. of the Second Int. Symp. on the Effects of Surface Geology on Seismic Motion*, Yokohama, Japan, 1-3 December 1998, Balkema, Rotterdam, 263-270.

Yegian, M. K., Ghahraman, V. G., and Gazetas, G., 1995, Soil amplification effect on building damage during the 1988 Armenia Earthquake, *Proc. of 10th European Conference on Earthquake Engineering*, Balkema, Rotterdam, 2621-2628.